

Gibberellin Metabolism and Transport During Germination and Young Seedling Growth of Pea (*Pisum sativum* L.)

Belay T. Ayele · Jocelyn A. Ozga ·
Aruna D. Wickramarathna ·
Dennis M. Reinecke

Received: 31 March 2011 / Accepted: 29 July 2011 / Published online: 27 September 2011
© Springer Science+Business Media, LLC 2011

Abstract The role of gibberellins (GAs) during germination and early seedling growth is examined by following the metabolism and transport of radiolabeled GAs in cotyledon, shoot, and root tissues of pea (*Pisum sativum* L.) using an aseptic culture system. Mature pea seeds have significant endogenous GA₂₀ levels that fall during germination and early seedling growth, a period when the seedling develops the capacity to transport GA₂₀ from the cotyledon to the shoot and root of the seedling. Even though cotyledons at 0–2 days after imbibition have appreciable amounts of GA₂₀, the cotyledons retain the ability to metabolize labeled GA₁₉ to GA₂₀ and express significant levels of *PsGA20ox2* message (which encodes a GA biosynthesis enzyme, GA 20-oxidase). The large pool of cotyledonary GA₂₀ likely provides substrate for GA₁ synthesis in the cotyledons during germination, as well as for shoots and roots during early seedling growth. The shoots and roots express GA metabolism genes (*PsGA3ox* genes which encode GA 3-oxidases for synthesis of bioactive GA₁, and *PsGA2ox* genes which encode GA 2-oxidases for deactivation of GAs to GA₂₉ and GA₈), and they develop the capacity to metabolize GAs as necessary for seedling establishment. Auxins also show an interesting pattern during early seedling growth, with higher levels of 4-chloro-indole-3-acetic acid (4-Cl-IAA) in mature seeds and higher levels of indole-3-acetic acid (IAA) in young

root and shoot tissues. This suggests a changing role for auxins during early seedling development.

Keywords Auxins · Gene expression · Gibberellin metabolism · Hormone transport · *Pisum sativum* · Seed germination · Seedling growth

Introduction

Plant hormones are chemical signal molecules that influence many aspects of plant growth and developmental processes. Mature seeds contain embryonic plants that are arrested in their development and that await the appropriate environmental conditions to initiate growth and development into seedlings. Gibberellins (GAs), in part, control the transition process of the embryo axis from quiescence to active growth. In small seeded plant species such as *Arabidopsis* and tomato, endogenous levels of GAs are a critical determinant for seed germination (radical protrusion). Severely GA-deficient mutants of *Arabidopsis* (*gal-3* and *ga2-1*) and tomato (*gib-1*) failed to germinate without exogenous GAs (Koornneef and van der Veen 1980; Groot and Karssen 1987), and embryos of the GA-deficient *gib-1* mutant of tomato showed a reduced growth rate (Groot and Karssen 1987), suggesting that the newly synthesized GAs are required for radicle protrusion in tomato and *Arabidopsis*. Subsequent growth of the young seedling requires an adequate level of bioactive GA to maintain vegetative growth (Koornneef and van der Veen 1980).

Pea (*Pisum sativum* L.) is a model legume for biochemical studies to understand factors that influence seed germination and early seedling growth in a larger nonendospermal seed. Early seedling growth in pea is promoted by GAs (Brian and Hemming 1955), but the role of

B. T. Ayele
Department of Plant Science, University of Manitoba, 222
Agriculture Building, Winnipeg, MB R3T 2N2, Canada

J. A. Ozga (✉) · A. D. Wickramarathna · D. M. Reinecke
Plant BioSystems, Department of Agricultural, Food and
Nutritional Science, 4-10 Agriculture/Forestry Centre,
University of Alberta, Edmonton, AB T6G 2P5, Canada
e-mail: jocelyn.ozga@ualberta.ca

bioactive GAs in germination has been questioned from the results of GA biosynthesis inhibitor studies. Experiments using the GA biosynthesis inhibitors that interfere with the cyclization of geranylgeranyl diphosphate (Sponsel 1983), oxidation of *ent*-kaurene to *ent*-kaurenoic acid (Graebe 1986), and 3 β -hydroxylation of GA₂₀ to GA₁ (Ross and others 1993; Ayele and others 2006b) suggested that de novo GA biosynthesis was not essential for pea seed germination, although it was necessary for the maintenance of normal seedling growth soon after germination. Bioactive GAs are positive effectors for growth in expanding shoots of plants, but their importance in root growth has been less obvious because external application of GA does not generally stimulate root elongation. Generally, only after treatment with GA biosynthesis inhibitors do roots respond in a dose-dependent fashion to GA application. For example, ancymidol, a GA biosynthesis inhibitor of *ent*-kaurene oxidase (an enzyme early in the GA biosynthesis pathway), inhibited shoot and root elongation in ‘Alaska’ seedlings (the cultivar used in the current study; Tanimoto 1988). Interestingly, the ancymidol-inhibited roots responded to lower concentrations of applied bioactive GA than ancymidol-inhibited shoots, supporting the hypothesis that roots require lower amounts of GA for optimal growth. Additionally, the severe pea GA-biosynthesis mutant *na* has low GA₁ levels in shoot and root tips, slower root and shoot growth, and increased growth in both organs upon treatment with bioactive GA (Yaxley and others 2001; Silva and Davies 2007). A role for GAs in early seedling growth for shoots and roots was suggested by these studies.

In pea plants, the later stages of GA biosynthesis occur mainly through the early 13-hydroxylation pathway: GA₁₂ → GA₅₃ → GA₄₄ → GA₁₉ → GA₂₀ → GA₁ (Sponsel 1995). The activities of three groups of GA oxidases (2-oxoglutarate-dependent dioxygenases) are critical in modulating the level of bioactive GA₁ (Hedden and Phillips 2000; Ozga and others 2009). These groups include GA 20-oxidases (which catalyze the synthesis of GA₅₃ to GA₂₀; encoded by *PsGA20ox1* and *PsGA20ox2*), GA 3 β -hydroxylases (which catalyze the conversion of GA₂₀ to bioactive GA₁; encoded by *PsGA3ox1* and *PsGA3ox2*), and GA 2 β -hydroxylases (which catalyze the conversion of GA₂₀ to biologically inactive GA₂₉, and also bioactive GA₁ to inactive GA₈; encoded by *PsGA2ox1* and *PsGA2ox2*). The expression pattern of genes encoding most of these enzymes and also the accompanying GA levels have been studied in both the growing embryo axis and in the nongrowing cotyledonary tissues during germination and subsequent young seedling growth of pea (Ayele and others 2006a). An exception is *PsGA3ox2*, which has only recently been isolated (Weston and others 2008). Ayele and others (2006a) observed that the initial imbibition of pea seeds resulted in decreased transcript abundance of GA catabolism genes

(*PsGA2ox1* and *PsGA2ox2*) and decreased levels of a product of 2 β -hydroxylation, GA₂₉. Additionally, cotyledons of imbibing seeds had an increased transcript abundance of three GA biosynthetic genes (*PsGA20ox1*, *PsGA20ox2*, and *PsGA3ox1*), as well as the production of GA₁ prior to radicle protrusion. The completion of germination, that is, at radicle protrusion through the seed coat (2 days after imbibition, DAI), was accompanied by a further increase in transcript abundance of cotyledonary *PsGA20ox2* and *PsGA3ox1*. A decrease in the endogenous levels of cotyledonary GA₂₀, GA₂₉, and GA₁ also occurred by 2 DAI and likely reflects turnover of these GAs within the cotyledonary tissue and/or transport of these GAs to the embryo axis. Furthermore, an attached embryo axis was required for stimulation of cotyledonary GA biosynthesis. As the embryo axis doubled in size, GA biosynthesis gene expression increased and GA catabolism gene expression decreased or remained low (Ayele and others 2006a).

The developmental capacity of pea cotyledons to transport GAs to the embryo axis prior to and following germination, and the role of GA metabolism in the regulation of biologically active GA levels in the cotyledons and embryo axis, are not known. Indirect evidence supports the postulation that GA₂₀ is transported from the cotyledons to the embryo axis where GA₁ synthesis then occurs and allows for embryo axis growth. For example, the *sln* mutant (*PsGA2ox1* mutation) has higher levels of GA₂₀ in the mature seed (230–380-fold higher) and produces long slender internodes during early seedling growth compared to wild-type seedlings (Reid and others 1992; Ross and others 1993). Application of prohexadione-Ca (an enzyme cofactor mimic which can inhibit the 3 β -hydroxylation of GA₂₀) to seeds prior to planting reduced elongation of the early internodes of *sln* plants by 73% (Ross and others 1993). In contrast, application of a GA biosynthesis inhibitor early in the pathway, paclobutrazol, which inhibits *ent*-kaurene oxidase, did not (Reid and others 1992). Furthermore, treatment of *SLN* seeds with GA₂₀ prior to planting resulted in a phenocopy of the *sln* plants with elongated basal internodes. However, direct evidence that demonstrates the transport of GA₂₀ from cotyledons to the embryo axis during normal seedling development is lacking.

Auxins are another class of plant hormone implicated in the processes of germination and early seedling growth (McDavid and others 1972; Ogawa and others 2003; Rampey and others 2004). Shoot growth is, in part, regulated by auxins (Rampey and others 2004; Dharmasiri and others 2005), and root growth is inhibited and root primordial initiation is stimulated by applied auxins (McDavid and others 1972; Wightman and others 1980). In *Arabidopsis*, an interaction of GA and auxin during seed germination was indicated from a study with GA-deficient *gal-3* seeds (Ogawa and others 2003). Here, application of a bioactive

GA treatment upregulated genes coding for auxin transporters as well as cytochrome P450s, the latter being involved in formation of IAA via indole-3-acetaldoxime. Developing seeds biosynthesize and accumulate free and conjugated auxins that can subsequently supply auxins for early growth of the seedling (Epstein and others 1980; Bialek and Cohen 1989; Rampey and others 2004). Pea plants have two naturally occurring auxins, IAA and 4-Cl-IAA, that promote pea internode elongation and fruit development, respectively, in part through their stimulation of the GA biosynthetic pathway (van Huizen and others 1997; Ross and others 2000; Ozga and Reinecke 2003; Ozga and others 2009). 4-Cl-IAA is generally a stronger auxin than IAA in stimulating excised shoot-section growth and inhibiting root growth (cited from Reinecke 1999). Thirteen-day-old pea shoot explants became weakly apically dominant and formed lateral roots following 4-Cl-IAA treatment ($1 \mu\text{M}$), whereas applied IAA stimulated root initiation at higher concentrations ($10 \mu\text{M}$) but did not affect apical dominance (Ahmad and others 1987). It was suggested that the loss of apical dominance was induced by increased ethylene evolution following 4-Cl-IAA treatment. Auxins IAA and 4-Cl-IAA have also been reported to be sequestered by conjugation to amino acids and proteins in mature seeds of pea (IAA and 4-Cl-IAA) and bean (IAA) (Bandurski and Schulze 1977; Magnus and others 1997; Park and others 2010). Such bound auxins in legume seeds could be released as free auxin upon enzyme hydrolysis for use during seed germination and early seedling growth processes (Bandurski and Schulze 1977). Schneider and others (1985) used gas chromatography-mass spectrometry (GC-MS) to identify and quantify IAA and to identify 4-Cl-IAA from 3-day-old etiolated pea epicotyls, roots, and cotyledons. However, a detailed analysis of the type, amount, and tissue location of auxins, especially 4-Cl-IAA, in the embryo from the mature seed to the young seedling stage has not been performed.

In the present study we investigated the dynamics of GA gene expression, metabolism, and transport during germination and early seedling growth in pea using qRT-PCR, radiolabeled GA tracer studies, and GC-MS quantitation of endogenous GA levels in shoots, roots, and cotyledons from aseptically cultured seedlings. Furthermore, we quantified two naturally occurring auxins of pea, IAA and 4-Cl-IAA, during these developmental stages to determine possible roles of these auxins in these processes.

Materials and Methods

Growth Assay

The pea (*Pisum sativum* L.) model cultivars used in this study were ‘Alaska’ (I₃), a tall vining green-seeded pea

with normal leaf morphology, and ‘Carneval,’ a semidwarf yellow-seeded field pea (*le-1*; single base-pair mutation in *PsGA3ox1*) with semileafless morphology (*af [afila]*, leaflets are replaced by tendrils of normal anatomy). Mature air-dried seeds of ‘Alaska’ (5.4% RWC [relative water content]) and ‘Carneval’ (5.8% RWC) were surface sterilized in 1.2% sodium hypochlorite solution for 25 min, rinsed five times with sterile deionized water, and then placed in a 9-cm sterile Petri plate (20 seeds per plate) on sterile Whatman #1 filter paper wetted with 10 ml of sterile deionized water. After 2 days of imbibition in darkness, the testa was removed and seedlings with typical shoot and root growth were aseptically transferred into a 15-cm sterile Petri plate (5 seedlings per plate) on sterile Whatman #1 filter paper wetted with 10 ml of sterile deionized water and covered with a second layer of filter paper. The plates were sealed with parafilm and then placed vertically (to obtain straight roots and shoots) in a growth chamber (Conviron, Asheville, NC) at 22/20°C (day/night) in a 16/8-h photoperiod with cool white fluorescent and incandescent lights ($205.5 \mu\text{E m}^{-2} \text{s}^{-1}$) until harvest. For growth measurements, seedlings of each cultivar were harvested from Petri plates at 2, 3, 4, 5, and 6 DAI and separated into cotyledons, roots, and shoots (7–10 seedlings per replication; 3 replications per time point). For RNA extraction and hormone analysis, 2 days after the transfer to the larger plates (4 DAI), seedlings were harvested, separated into shoots, roots, and cotyledons, and immediately frozen in liquid N₂ and stored at -80°C . Seed germination and seedling growth conditions for comparing the expression of *PsGA3ox1* and *PsGA3ox2* genes in tissues from 0 to 6 DAI were the same as described previously (Ayele and others 2006a). To analyze gene expression and endogenous hormone levels in the mature embryo (cotyledon and embryo axis combined), seeds of the two cultivars were immersed in ice:water (1:1, w/v) for 4 h to facilitate seed coat removal, and the embryos were immediately frozen in liquid N₂ and stored at -80°C until extraction for total RNA or hormone analysis.

Shoot and Root Morphology Studies

For assessment of lateral shoot branching, mature air-dried seeds of the two cultivars were planted at a depth of approximately 2.5 cm in 3-L plastic pots containing a 1:1 ratio of sand:Metro-Mix (W.R. Grace and Co., Toronto, Canada) (6 seeds per pot, 3 pots per cultivar), and the pots were placed in a growth chamber with conditions as described above. The number of lateral branches per shoot was assessed 1 month after planting. To assess the role of the shoot on growth and morphology of the root, seedlings of both cultivars were cultured aseptically as described above. After 2 days of imbibition in darkness in the 9-cm

sterile Petri plate culture, seedlings were decapitated by surgically removing the plumules without damaging the cotyledons (control plants were left intact) prior to transfer into the 15-cm sterile Petri plates (6 seedlings per plate). Decapitated seedlings of both ‘Alaska’ and ‘Carneval’ were either untreated or treated with IAA or 4-Cl-IAA (1 μM or 10 μM in 0.1% Tween-80 solution, 1 μl applied directly to the stump) daily until harvest (6 DAI, with the first treatment started immediately after decapitation). To investigate the effect of shoot-derived GA on root response to IAA, decapitated seedlings of ‘Carneval’ (*le-1*) were treated with IAA plus GA₃ or with 4-Cl-IAA plus GA₃ (10 μM in 0.1% Tween-80 solution, 1 μl applied to the stump). After treatment, all Petri plates were placed in a growth chamber environment as described above. One set of decapitated seedlings of ‘Carneval’ were also kept in darkness until harvest.

RNA Isolation

Tissues were finely ground in liquid N₂ and used for RNA isolation following a modified TRIzol (Invitrogen, Carlsbad, CA) protocol as described previously by Ayele and others (2006a). The RNA fraction was subjected to further extraction with chloroform (0.2 ml ml⁻¹ TRIzol), subsequently precipitated by using isopropanol (0.25 ml ml⁻¹ TRIzol) and high salt solution (1.2 M Na citrate and 0.8 M NaCl), 4 M LiCl, and finally by a mixture of 3 M Na acetate (pH 5.2):100% ethanol (1:20, v/v). The precipitate was dissolved in DEPC-treated water. Verification of the RNA integrity, DNase digestion of the total RNA samples, purification of the seed and cotyledonary total RNA samples, and determination of RNA concentrations was performed as described previously (Ayele and others 2006a).

Gene Expression Analysis

Primers and Probes

Primers and probes for the quantifying amplicons (*GA20ox1-104* and *GA20ox2-88*, *GA3ox1-87*, *GA3ox2-104*, *GA2ox1-73* and *GA2ox2-83*, and *18S62*) of the target genes (*PsGA20ox1* and *PsGA20ox2*, *PsGA3ox1*, *PsGA3ox2* and *PsGA2ox1*, and *PsGA2ox2*) and reference gene (pea 18S rRNA) were designed as described previously (Ayele and others 2006a; Ozga and others 2009).

Real-Time RT-PCR Assay

Real-time RT-PCR assays were performed on an Applied Biosystems (ABI, Foster City, CA) StepOnePlus sequence detector (for *PsGA3ox1* and *PsGA3ox2* quantitation) or on

an ABI model 7700 sequence detector (quantitation of all other genes) using a TaqMan One-Step RT-PCR Master Mix Reagent Kit (Applied Biosystems) as 25- or 50- μl reactions as described previously (Ayele and others 2006a). Thermal cycling conditions were 48°C for 30 min for RT, 95°C for 10 min for *Taq* activation, and 40 cycles of 95°C for 15 s and 60°C for 1 min for PCR. Total RNA extracts from each tissue were pooled across all time points per cultivar, and this pooled sample was run on each plate and used as a control to correct for plate-to-plate amplification differences. A pooled sample in one real-time RT-PCR run was taken as the standard arbitrarily and used for normalizing the C_t values of samples in other runs as described previously (Ayele and others 2006a). The average of two assays of each sample was used to determine the relative transcript abundance of each target gene using the 2^{- ΔC_t} method (Livak and Schmittgen 2001).

Extraction and Partitioning of Endogenous Auxin and GA

Mature embryos (cotyledon plus embryo axis), cotyledons, shoots, or roots (approximately 20 g fresh weight [gfw] per sample) were ground to a fine powder in a precooled mortar and pestle, in liquid N₂. The fine powder was then homogenized with cold 80% (v/v) aqueous methanol containing 10 mg l⁻¹ butylated hydroxytoluene (10 ml gfw⁻¹). The stable isotope-labeled GAs [²H]GA₁ (300 ng), [²H]GA₈ (300 ng), [²H]GA₁₉ (300 ng), [²H]GA₂₀ (291.9 ng), and [²H]GA₂₉ (300 ng) (obtained from L.N. Mander, Australian National University) and the stable isotope-labeled auxins [²H₄]4-Cl-IAA and [¹³C₆]IAA (obtained from J. Cohen, University of Minnesota and Cambridge Isotope Laboratories, respectively) were added at homogenization of each extract as internal standards for recovery determination at the GC-MS step. The plant material was extracted overnight twice on a shaker (100 rpm) at 4°C in darkness. The extracts were then centrifuged for 30 min at 10,000 $\times g$, and the methanolic extracts were pooled and evaporated to the aqueous phase using a SpeedVac concentrator (Savant, Farmingdale, NY) without supplemental heating. The aqueous phase was then filtered through silylated glasswool, adjusted to pH 8 with 0.1 N NH₄OH, and partitioned four times against *n*-hexane (5 ml). The aqueous phase was then adjusted to pH 3 with 0.1 N HCl and partitioned five times against ethyl acetate (5 ml). The combined ethyl acetate extract was reduced in volume using the SpeedVac concentrator, and hexane was added to drive off any acid residue. The reduced ethyl acetate extract was partitioned four times against 5% (w/v) aqueous NaHCO₃ (2 ml). The pH of the combined NaHCO₃ extract was adjusted to pH 3 with 6 N HCl on ice, and then partitioned four times against ethyl

acetate (5 ml). The ethyl acetate extracts were pooled and evaporated to complete dryness using the SpeedVac concentrator. The ethyl acetate extract residue was then dissolved in H₂O (1 ml), loaded onto a Bond Elut C₁₈ column (1 g; Varian Inc., Harbor City, CA) that was preconditioned with methanol (2 ml) followed by H₂O (2 ml). The column was then washed with H₂O (2 ml) and eluted with MeOH (4 ml). The MeOH eluates were pooled, evaporated to dryness, resuspended in MeOH (1 ml), and loaded onto a Bond Elut DEA column (500 mg; Varian) that was preconditioned with MeOH (5 ml). The Bond Elut DEA column, which had a head of DEAE-Sephacel (1 ml of gel suspended in EtOH), was then eluted with 1 N AcOH in MeOH (5 ml). The eluates of the 1 N acetic acid in MeOH were combined and dried completely using the SpeedVac concentrator (hexane was added in the drying process to eliminate residual acetic acid) prior to high-pressure liquid chromatography (HPLC) purification.

GA Metabolism and Transport

To study the dynamics of GA metabolism in the cotyledons and embryo axes of germinating seeds, and GA transport from the cotyledons to the embryo axis/shoot and root or from the shoot to the root, seeds of ‘Alaska’ were surface sterilized and imbibed in a 9-cm sterile Petri plate prior to transfer into a 15-cm Petri plate culture as described above. 17-¹⁴C]GA₁₉ (specific activity of 54 μCi μmol⁻¹; a total of ca. 72,964 disintegrations per min (dpm) in 2 μl of 50% aqueous ethanol) or 17-¹⁴C]GA₂₀ (specific activity of 34 μCi μmol⁻¹; a total of ca. 82,000 dpm in 2.5 μl of 50% aqueous ethanol) was injected into one cotyledon of 1-, 2-, 3-, and 4-DAI seedlings of ‘Alaska’ at two different loci. The treated seedlings were harvested onto dry ice 12 h after injection of ¹⁴C]GAs and then separated into ¹⁴C]GA-treated and -untreated cotyledons, roots, and shoots. In an additional experiment, 2- and 4-DAI cotyledons were similarly treated and incubated with ¹⁴C]GA₂₀ for 6, 12, 24, and 48 h prior to harvest. To investigate GA metabolism in the embryo axis of germinating pea seeds, ¹⁴C]GA₁₉ (a total of 1.5 μl of 50% aqueous ethanol; a total of ca. 54,723 dpm), ¹⁴C]GA₂₀ (a total of 1.5 μl of 50% aqueous ethanol; a total of ca. 48,000 dpm), or 17-¹⁴C]GA₁ (specific activity of 34 μCi μmol⁻¹; a total of ca. 44,140 dpm in 2 μl of 50% aqueous ethanol) was applied to the surface of the embryo axis at 0.5, 1, and 2 DAI. The treated embryo axes were harvested onto dry ice 12 h after ¹⁴C]GA application.

To examine GA transport from the cotyledon to the axis tissues of pea seedlings, 17-¹⁴C]GA₂₀ (specific activity of 34 μCi μmol⁻¹; a total of ca. 82,000 dpm in 2.5 μl of 50% aqueous ethanol) was injected into one cotyledon of 4-DAI seedlings of ‘Alaska’ at two different loci (Table 5). The

treated seedlings were harvested onto dry ice at 12, 24, and 48 h after injection of ¹⁴C]GA and then separated into ¹⁴C]GA-treated and -untreated cotyledons, roots, and shoots. To confirm the transport of GA from cotyledons to the axis tissues, another labeled substrate, [³H]GA₂₀ (specific activity of approximately 21 Ci mmol⁻¹ with the fraction of labeled GA remaining at ~70%), was injected into one of the cotyledons at 4 DAI after the other one was removed (Table 6). The treated seedlings were harvested and separated into cotyledons, roots, and shoots at 12 and 24 h after injection of [³H]GA₂₀.

To investigate the possible transport of GA from the shoot to root tissues of actively grown pea seedlings, 17-¹⁴C]GA₂₀ (specific activity of 34 μCi μmol⁻¹; a total of ca. 82,000 dpm in 2.5 μl of 50% aqueous ethanol) was applied to the surface of the shoot at 4 DAI (Table 7). The root and shoot tissues of the seedlings were harvested onto dry ice at 12 h after treatment with ¹⁴C]GA₂₀. All tissues were stored at -80°C until extraction.

The ¹⁴C]GA-treated and -untreated cotyledon halves, embryo axes, roots, and shoots (5 tissues per sample) were homogenized in cold 80% (v/v) methanol (10 ml per sample) using a polytron homogenizer in silylated 30-ml Corex tubes. 17-¹⁴C]GA₇ (ca. 11,000 dpm) was added at homogenization of each sample as an external standard for recovery determination of radioactive metabolites at the HPLC step. The extracts were shaken overnight on a shaker (150 rpm) at 4°C in darkness, and then centrifuged for 30 min at 10,000×g. The methanolic supernatant was removed, and the residue was resuspended in 5 ml of homogenization solvent and shaken for at least 4 h. The residue extracts were centrifuged for 30 min at 10,000×g, and the pooled methanolic extracts were evaporated to the aqueous phase using a SpeedVac concentrator. The aqueous extracts were solvent partitioned (after adjustment to the appropriate pH) sequentially with *n*-hexane, ethyl acetate, aqueous NaHCO₃, and ethyl acetate as described above. The final ethyl acetate extracts were pooled and evaporated to complete dryness using a SpeedVac concentrator prior to HPLC purification.

High-Performance Liquid Chromatography

The ethyl acetate extract residues were dissolved in 400 μl of 20% (v/v) MeOH, filtered through a 0.45-μm nylon filter (Whatman International Ltd., Maidstone, UK), and injected onto a 4.6 × 250-mm Spherisorb C₁₈ column (5 μm; Beckman Instruments Inc., Fullerton, CA). The samples were eluted at 1 ml min⁻¹ using the following linear gradient of methanol (solvent A) and 0.01% (v/v) aqueous TFA (solvent B): 20% (v/v) solvent A for 1 min, gradient to 100% (v/v) solvent A in 45 min, and isocratic 100% solvent A for 5 min. Radioactivity in the effluent of samples from the

[^{14}C]GA metabolism and transport studies was monitored using a flow-through radiochemical detector (Beckman 171). Fractions from the endogenous GA study and the [^{14}C] metabolism and transport studies, eluting at the retention times of GA₈ (9.6 min), GA₂₉ (10.7 min), GA₁ (16.1 min), GA₂₉-catabolite (16.4 min), IAA (17.8 min), 4-Cl-IAA (23.3 min), GA₂₀ (24.2 min), and GA₁₉ (27.4 min), were collected and reduced to dryness using a SpeedVac concentrator. For the [^{14}C]GA metabolism studies, pooled samples of the putative [^{14}C]GAs were methylated using diazomethane and rechromatographed on C₁₈ HPLC (using the same solvent system) to further confirm GA identity [retention times for GA-MEs were GA₈-ME (13.7 min), GA₂₉-ME (16.5 min), GA₁-ME (18.5 min), GA₂₉-catabolite-ME (24.6 min), and GA₂₀-ME (27.0 min)]. For the [^3H]GA₂₀ transport study, fractions eluting at the retention times of the GA standards were collected, and the amount of radioactivity present in each collected fraction was determined directly using a Beckman 5801 liquid scintillation counter. The putative identities of the [^{14}C]GA metabolites from this study with pea seedlings are based on results from the metabolism profiles from three GA substrates and from HPLC analysis of the metabolites as the free and methyl esters as compared to known GA standards. The identity of the [^{14}C]GA and [^3H]GA metabolites awaits further confirmation by mass spectrometry. Previously, the identities of the radiolabeled GA₈ and GA₂₉ metabolites from 4-day-old cotyledons fed [^{14}C]GA₂₀ were confirmed by GC-MS by retention time and characteristic fragment ions as the trimethylsilyl (TMS) derivatives of GA₈-ME and GA₂₉-ME (Ayele and others 2006a).

Gas Chromatography-Mass Spectrometry

HPLC fractions containing putative endogenous GAs, IAA, and 4-Cl-IAA were resuspended in 100 μl of 100% (v/v) methanol and methylated by dropwise addition of diazomethane and incubation for 20 min at room temperature. The methylation step was repeated for a second time to ensure completion of the reaction. The solvent was evaporated under N₂ at 40°C. Conversion of the methylated samples to their methyl ester-trimethylsilyl ether derivatives was performed according to Gaskin and MacMillan (1991). The dried sample was taken up in 50 μl of pyridine and a 15 μl mixture of pyridine, hexamethyldisilazane, and trimethylchlorosilane in the ratio of 5:6:4. The tightly capped vial was incubated at 100°C for 10 min followed by drying in a stream of N₂ at 40°C. The sample residue was then brought up in 20 μl of dichloromethane (DCM) and 10 μl of *N*-methyl-*N*-trimethylsilyltrifluoroacetamide (MSTFA), tightly capped, and heated to 100°C for 45 s to dissolve the NH₄Cl. The silylated samples were stored in a desiccator over P₂O₅ at room temperature prior to GC-MS injection. After removal

of the MSTFA and DCM under a stream of N₂ at 40°C, the sample was brought up in 5 μl of dry redistilled DCM prior to injection onto a Hewlett–Packard model 5890 series II *plus* gas chromatograph interfaced to a Hewlett–Packard model 5972A mass selective detector. Samples (1 μl) were injected on-column onto a HP-5 MS capillary column (30 m \times 0.25 mm \times 0.25 μm film thickness; J&W Scientific Inc., Folsom, CA) with an initial column temperature at 50°C for 2 min followed by temperature programming at 10°C min⁻¹ to 150°C, and then 3°C min⁻¹ to 300°C. Helium was used as the carrier gas at a flow rate of 1 ml min⁻¹. Hormones were identified by selected ion monitoring (SIM) of three prominent ions (including the molecular ion M⁺) characteristic to the corresponding hormone. In addition, a solution of *n*-alkanes was coinjected with the samples, and retention times of the respective *n*-alkane peaks were recorded to obtain the Kovats Retention Index (KRI) values for further confirmation of the identity of the GAs studied. Endogenous hormone levels were calculated according to Gaskin and MacMillan (1991) where the protio- and deutero-ions monitored were corrected for the donation of natural isotopes to the peak area and quantification was based on the most prominent ion measured: protio-IAA-Me-TMS (202 ion); protio-4-Cl-IAA-Me-TMS (236 ion); protio-GA₁₉-Me-TMS (434 ion; KRI, 2627); protio-GA₂₀-Me-TMS (418 M⁺; KRI, 2561); protio-GA₁-Me-TMS (506 M⁺; KRI, 2710); protio-GA₈-Me-TMS (594 M⁺; KRI, 2840); and protio-GA₂₉-Me-TMS (506 M⁺; KRI, 2717).

Results and Discussion

Seedling Growth

The growth dynamics of ‘Alaska’ and ‘Carneval’ seedlings were assessed in a Petri plate system (Fig. 1a) optimized for transport and metabolism studies in an aseptic growth environment. Root growth in fresh weight and length was linear except for ‘Carneval’ fresh weight, which slowed by 5 and 6 DAI. Root growth was greater than shoot growth from 2 through 6 DAI in both cultivars when grown in the aseptic Petri plate system (Fig. 1b) or in sand culture (Ayele and others 2006a). Shoot growth was slower from 2 to 4 DAI and gradually increased from 4 to 6 DAI (Fig. 1d, e). Shoot growth was lower (approximately ninefold for fresh weight and fivefold for length) for the Petri plate-cultured seedlings of both cultivars (Fig. 1d, e) than those cultured in sand (Ayele and others 2006a). Root growth of both cultivars was also lower (approximately three- to fourfold in fresh weight) in the Petri plate-cultured seedlings (Fig. 1b) than those from the sand culture. However, the root length of both cultivars was affected to a lesser extent by the culture system [only 1.8-fold lower in those

cultured in a Petri plate (Fig. 1c) as compared to the sand-grown seedlings (Ayele and others 2006a)]. The observed difference in growth between the seedlings from the two culturing systems was due in part to different light conditions between these systems, as the seedlings cultured in the Petri plate system were transferred to light (16 h day/8 h night) after the completion of germination, that is, 2 DAI, whereas only the elongating shoot from the sand system was exposed to light after emergence from the soil (5 DAI; Ayele and others 2006a). A number of studies that involved the use of etiolated pea seedlings have demonstrated that light inhibits stem elongation (white light, including fluorescent light as was used in the current study, red light, and blue light) within hours of treatment (Behringer and Davies 1993). Growing the seedlings aseptically in the dark following transfer to the large Petri plate increased the shoot and root fresh weights by 128 and 25%, respectively, as compared to the aseptically cultured seedlings transferred to a large Petri plate and grown in the light (data not shown).

[¹⁴C]GA Metabolism in the Cotyledons of Germinating Pea Seeds

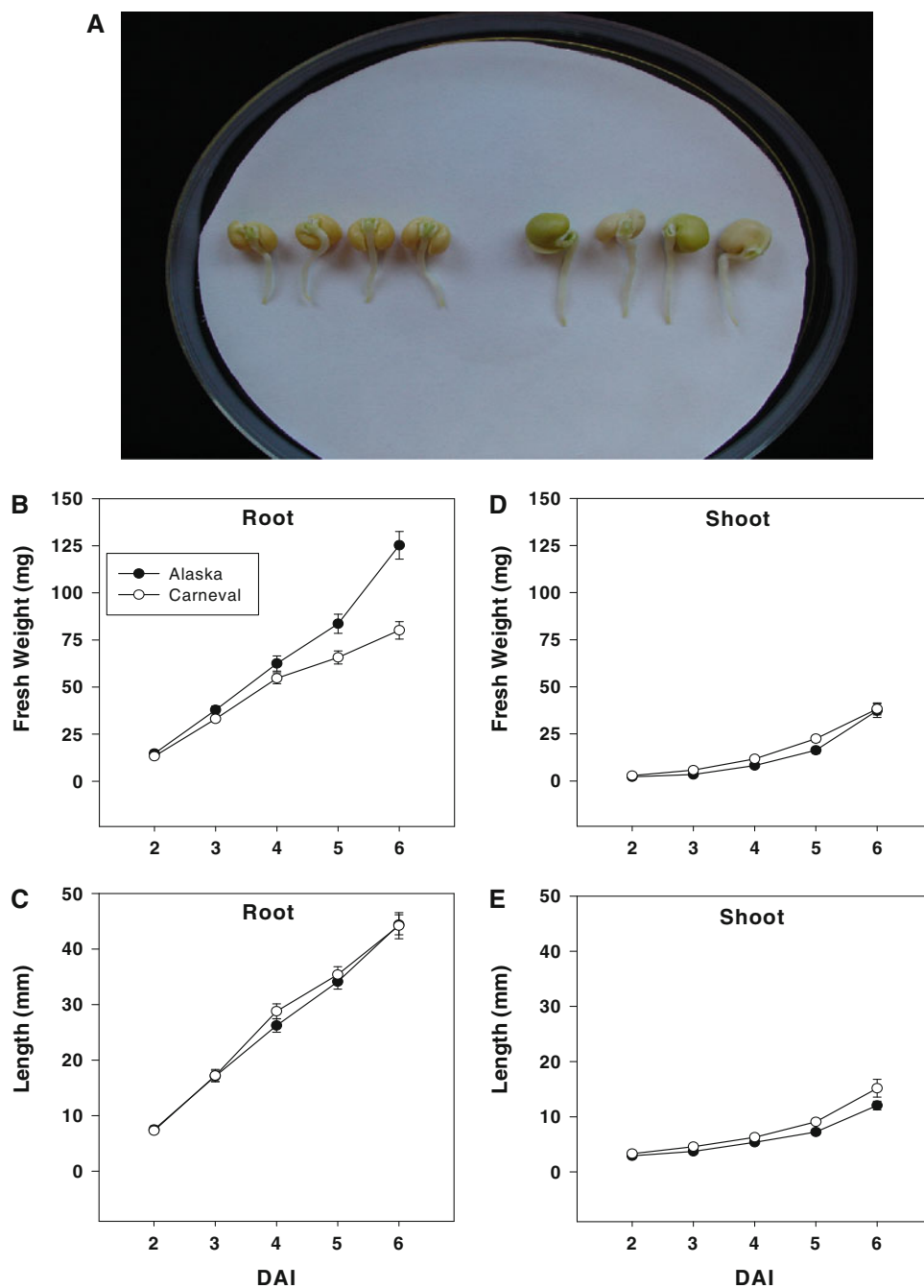
The dynamics of GA metabolism in the cotyledons of germinating pea seeds were studied using radiolabeled GA substrates with ‘Alaska’ seeds and seedlings in the aseptic Petri plate culture system (Fig. 1a). The observed radiolabeled GA metabolites were preliminarily identified by their HPLC retention times as their free and methyl esters in comparison to GA standards and await further confirmation by GC-MS analysis (Ayele and others 2006a). Cotyledons of imbibing pea seeds treated at 1, 2, 3, or 4 DAI were able to convert [¹⁴C]GA₁₉ to [¹⁴C]GA₂₀, with the highest production of [¹⁴C]GA₂₀ observed at 3 DAI (Table 1). This metabolism profile is consistent with an increase in *PsGA20ox2* transcript abundance in 2-DAI ‘Alaska’ cotyledons (Ayele and others 2006a), and higher levels of *PsGA20ox2* at 2 DAI than at 4 DAI in cotyledons for Petri plate-grown seedlings (Table 2). The metabolism and gene expression data indicate that the pool of GA₂₀ in the cotyledons of imbibing seeds may include GA₂₀ from de novo biosynthesis as well as GA₂₀ sequestered during seed development (see GA levels subsection).

When 2-DAI cotyledons were injected with [¹⁴C]GA₂₀, within 6 h of application approximately 83% of the labeled substrate was either metabolized and/or transported from the cotyledonary tissue, of which 19% was converted into [¹⁴C]GA₈, [¹⁴C]GA₂₉, and [¹⁴C]GA₂₉-catabolite (Fig. 2). Although minimal to no [¹⁴C]GA₁ was detected as a metabolite in this experiment, its immediate metabolite [¹⁴C]GA₈ was detected within 6 h of application (approximately 9% of the [¹⁴C]GA₂₀ applied into the cotyledon).

By 12 h of incubation with [¹⁴C]GA₂₀, [¹⁴C]GA₈ increased threefold (to approximately 26% of the [¹⁴C]GA₂₀ applied into the cotyledon) and was the major [¹⁴C]GA metabolite detected at this time (Fig. 2d). However, minimal conversion of [¹⁴C]GA₂₀ to [¹⁴C]GA₈ occurred in 4-DAI cotyledons (Fig. 2d). A subsequent [¹⁴C]GA₂₀ metabolism experiment with 1-, 2-, 3-, and 4-DAI cotyledons confirmed this metabolic pattern because conversion of [¹⁴C]GA₂₀ through to [¹⁴C]GA₈ was maximal in 2-DAI cotyledons (highest [¹⁴C]GA₈ levels for all three replicate samples) and minimal at 4 DAI (Table 1). These metabolism data are consistent with a peak in endogenous GA₁ observed in the cotyledons during germination (1 DAI) followed by minimal to no detectable GA₁ in the cotyledons following germination (Ayele and others 2006a) (Table 3). Interestingly, 2-DAI cotyledons required the presence of the attached embryo axis for maximum *GA3ox1* expression and also for metabolism of radiolabeled GA₂₀ to GA₈ (Ayele and others 2006a). Cotyledonary *PsGA3ox1* transcript abundance increased prior to germination (from 0.5 to 2 DAI; Fig. 3f). However, a direct relationship between cotyledonary *PsGA3ox* transcript levels, [¹⁴C]GA metabolism profiles, and endogenous GA levels was not evident at 4 DAI when the transcript abundance of *PsGA3ox1* peaked (Fig. 3f; Table 2), although little to no conversion of labeled GA₂₀ (through GA₁) to GA₈ and relatively low endogenous levels of GA₁ were observed (Tables 1, 3). After 2 DAI, the post-transcriptional or post-translational regulation of cotyledonary *PsGA3ox* or GA 3-oxidase, respectively, may reduce production of bioactive GA₁.

High levels of *PsGA2ox* mRNA and conversion of [¹⁴C]GA₂₀ to [¹⁴C]GA₂₉ (up to 12% of the [¹⁴C]GA₂₀ applied to the cotyledon within 48 h of incubation) were evident for 2-DAI cotyledons (Fig. 2; Tables 1, 2, ‘Alaska’). At 4 DAI, cotyledons converted [¹⁴C]GA₂₀ to mainly [¹⁴C]GA₂₉, with little to no conversion of [¹⁴C]GA₂₀ through to [¹⁴C]GA₈ (Fig. 2; Table 1). The 4-DAI metabolic profile is in agreement with the accumulation of endogenous GA₂₉ (with minimal to nondetectable levels of GA₁ and GA₈; Table 3, ‘Alaska’) and *PsGA2ox* mRNA expression (Table 2, ‘Alaska’ cotyledon). These data support a role for 2β-hydroxylation in modulating the content of bioactive GA in this tissue during germination and early seedling growth. We would like to note that the metabolic profiles of the [¹⁴C]GA₁₉ and [¹⁴C]GA₂₀ cotyledonary metabolism studies (Table 1) vary because when using [¹⁴C]GA₁₉ as the applied GA substrate, the amount of [¹⁴C]GA₂₀ produced and available for conversion to [¹⁴C]GA₁ and then [¹⁴C]GA₈ is small compared to that available in the [¹⁴C]GA₂₀-fed tissues. The substantially higher levels of [¹⁴C]GA₂₀ in the [¹⁴C]GA₂₀-fed tissue also leads to greater levels of [¹⁴C]GA₂₉ than that in [¹⁴C]GA₁₉-fed tissues.

Fig. 1 Growth of seedlings of ‘Carneval’ and ‘Alaska’ in a Petri plate system. Four day-old seedlings of ‘Carneval’ (*left four*) and ‘Alaska’ (*right four*) (a). Root fresh weights (b) and length (c), and shoot fresh weight (d) and length (e) from 2 to 6 DAI. Data are mean \pm SE, $n = 24$ to 30



Overall, these data suggest that the cotyledons of germinating pea seeds convert GA_{20} to bioactive GA_1 followed by deactivation of GA_1 by 2β -hydroxylation to GA_8 during or immediately after radicle protrusion, a time when the procambium differentiates into vascular tissue in the cotyledons (Smith and Flinn 1967). Because GA treatment increased the transcript abundance of *PsPIN1*, a putative auxin efflux carrier, in pea stems (Chawla and DeMason 2004), we would speculate that cotyledonary GA_1 may be involved in vascular development in the cotyledons by modulating the expression of auxin efflux

carriers, and in turn localization of auxin resulting in vascular differentiation. It is also possible that GA_1 produced in the cotyledons may have a role in triggering the expression of GA -inducible cotyledonary genes encoding cell-wall-loosening enzymes (Chen and others 2001; Ogawa and others 2003), which may take part in the formation of a large reticulum of intercellular spaces observed during germination of pea seeds (Smith and Flinn 1967), with a possible function of accommodating high respiratory activity during reserve mobilization (Bain and Mercer 1966). These radioactive metabolism data also

Table 1 [¹⁴C]GA metabolites in the cotyledons of ‘Alaska’ after 12 h of incubation with [¹⁴C]GA₁₉ or with [¹⁴C]GA₂₀

DAI	[¹⁴ C]GA ₂₀	[¹⁴ C]GA ₁	[¹⁴ C]GA ₂₉	[¹⁴ C]GA ₂₉ -catabolite	[¹⁴ C]GA ₈
[¹⁴C]GA Metabolite after 12 h of incubation with [¹⁴C]GA₁₉					
1	2.0 ± 0.1 ^a (7,179 ± 278) ^c	0.2 ^b (890)	2.2 ± 0.2 (8,093 ± 848)	0.7 ^b (2,648)	nd
2	2.7 ± 0.7 (9,882 ± 2,696)	0.9 ^b (3,259)	2.2 ± 0.4 (8,158 ± 1,358)	2.0 ^b (7,526)	nd
3	5.5 ± 1.9 (19,923 ± 6,800)	0.9 ^b (3,439)	1.2 ± 0.3 (4,296 ± 1,248)	1.5 ± 0.9 (5,382 ± 3,238)	nd
4	2.5 ± 1.1 (8,933 ± 4,136)	0.5 ^b (1,941)	1.4 ± 0.8 (5,069 ± 2,862)	3.1 ± 2.3 (11,256 ± 8,256)	nd
[¹⁴C]GA Metabolite after 12 h of incubation with [¹⁴C]GA₂₀					
1		0.4 ^b (1,643)	14.8 ± 0.6 (60,271 ± 2,306)	nd	33.3 ^b (135,827)
2		nd	6.7 ± 0.9 (27,152 ± 3,824)	1.9 ^b (7,637)	26.1 ± 11.6 (106,483 ± 47,331)
3		0.5 ^b (2,030)	6.4 ± 4.2 (26,294 ± 17,143)	nd	nd
4		nd	16.5 ± 2.6 (67,189 ± 10,700)	0.7 ± 0.2 (2,667 ± 978)	0.5 ± 0.3 (2,068 ± 1,149)

The radiolabeled GA₁₉ or GA₂₀ was injected into one cotyledon of the seedling at 1, 2, 3, or 4 days after imbibition (DAI)

nd not detected

^a Values are percentages calculated as (dpm [¹⁴C] metabolite after 12 h of incubation)/(dpm [¹⁴C]GA substrate applied to the cotyledon) × 100. Data are mean ± SE (n = 3; 5 cotyledons per n)

^b [¹⁴C]GA metabolite was observed in only one of the three biological replicates

^c Values in parentheses are [¹⁴C] metabolite in dpm

confirm our previous hypothesis that the production of bioactive GA₁ in the cotyledons of young pea seedlings is limited to a short duration during germination and early seedling growth (Ayele and others 2006a).

[¹⁴C]GA Metabolism in the Embryo Axis of Germinating Pea Seeds

The dynamics of GA metabolism in the embryo axis was assessed during germination and immediately after the completion of germination (from 0.5 to 2 DAI) in ‘Alaska’ using [¹⁴C]GA₁₉, [¹⁴C]GA₂₀, and [¹⁴C]GA₁ as substrates. Consistent with a peak in *PsGA20ox1* transcript abundance in the 1-DAI embryo axis (Ayele and others 2006a), the conversion of [¹⁴C]GA₁₉ to [¹⁴C]GA₂₀ peaked at 1 DAI (Table 4), indicating a possible increase in the capacity of the embryo axis to produce GA₂₀. The ability to produce high levels of this immediate precursor of GA₁ may be necessary for initial embryo axis growth prior to vascularization of the cotyledon (procambium differentiation into vascular tissue by 2 DAI; Smith and Flinn 1967) and before significant transport of GA₂₀ from the cotyledon. *PsGA3ox1* and *PsGA3ox2* transcript abundance increased in the embryo axis prior to radical protrusion through the seed coat (sand-grown ‘Alaska’; Fig. 3e), and conversion of [¹⁴C]GA₂₀ to [¹⁴C]GA₁ was detected in embryo axes prior to this event (0.5 DAI in the Petri plate system;

Table 4). Although [¹⁴C]GA₁ was not detected in 1- and 2-DAI embryo axes treated with [¹⁴C]GA₂₀, the axes presumably made low levels of labeled GA₁ because [¹⁴C]GA₈ was observed at both time points. Catabolism of [¹⁴C]GA₂₀ to [¹⁴C]GA₂₉ occurred in embryo axes at 1 DAI when production of [¹⁴C]GA₂₀ from applied [¹⁴C]GA₁₉ was high, and from 0.5 to 2 DAI, peaking at 1 DAI, when embryo axes were fed [¹⁴C]GA₂₀ (Table 4). Overall, the [¹⁴C]GA metabolic profile observed with the embryo axis indicates that the expanding embryo axis has increased GA₂₀ and bioactive GA₁ synthesizing capacity by the time of radicle protrusion. Speculatively, the GA₁ synthesized by the embryo axis could be involved in triggering the expression of GA-inducible cell-wall-loosening enzymes that are responsible for cell elongation (Chen and others 2001; Ogawa and others 2003) in this tissue.

GA Transport from the Cotyledon into the Embryo Axis

GA transport from the cotyledons to the embryo axis of aseptically cultured ‘Alaska’ seedlings at 4 DAI (Fig. 1a) was studied by injecting one of the cotyledons with [¹⁴C]GA₂₀ or [³H]GA₂₀ and measuring transport of radioactive GAs into the growing embryo axis. A minimal amount of [¹⁴C]GA₂₀ was detected in shoot tissues 12 h after application to a cotyledon (in 1 of 3 replicates),

Table 2 Relative transcript levels of *PsGA20ox1*, *PsGA20ox2*, *PsGA3ox1*, *PsGA2ox1*, and *PsGA2ox2* in 2-DAI cotyledons of ‘Alaska’ and in the cotyledons, shoots, and roots of 4-DAI seedlings of ‘Alaska’ and ‘Carneval’ grown in a Petri plate

Gene	2 DAI	4 DAI		
	Cotyledon	Cotyledon	Shoot	Root
‘Alaska’				
<i>PsGA20ox1</i> ^a	58.0 ± 20.7 ^b	2.9 ± 1.3	1,930.5 ± 102.5	1,653.6 ± 577.9
<i>PsGA20ox2</i> ^a	39,730.0 ± 13,507.6	499.1 ± 60.6	194.4 ± 89.2	745.3 ± 260.1
<i>PsGA3ox1</i> ^a	0.4 ± 0.1	187.1 ± 49.6	31,738.3 ± 2,587.5	34,755.0 ± 856.0
<i>PsGA2ox1</i> ^a	128,036.7 ± 23,649.8	22,670.9 ± 1,860.5	5,583.5 ± 439.5	5,710.4 ± 605.0
<i>PsGA2ox2</i> ^a	17,287.8 ± 3,906.8	20,110.3 ± 5,929.0	1,083.9 ± 219.7	3,418.9 ± 330.2
<i>PsGA3ox1</i> ^c	1.2 ± 0.1	56.8 ± 9.4	9,869.0 ± 1,206.2	10,662.3 ± 1,021.3
<i>PsGA3ox2</i> ^c	1.0 ± 0.0	13.0 ± 1.2	235.0 ± 17.9	44.0 ± 2.9
‘Carneval’				
<i>PsGA20ox1</i> ^a		1.0 ± 0.2	1,004.0 ± 299.1	685.3 ± 191.1
<i>PsGA20ox2</i> ^a		123.4 ± 14.9	136.8 ± 34.3	582.3 ± 128.3
<i>PsGA3ox1</i> ^a		52.8 ± 19.7	14,595.9 ± 2,118.7	13,791.5 ± 2,139.8
<i>PsGA2ox1</i> ^a		3,676.5 ± 467.4	3,830.1 ± 775.7	6,762.7 ± 1,339.0
<i>PsGA2ox2</i> ^a		415.2 ± 102.7	358.5 ± 60.6	1,934.0 ± 348.4
<i>PsGA3ox1</i> ^c		23.2 ± 6.3	5,892.5 ± 677.6	3,351.3 ± 762.8
<i>PsGA3ox2</i> ^c		31.6 ± 8.2	43.3 ± 3.1	43.0 ± 2.7

^a Transcript levels were compared across genes, genotypes, and tissues using the average of cotyledonary *PsGA20ox1* samples of ‘Carneval’ as a reference for normalization. Quantitation was performed using an ABI 7700 sequence detector

^b Data are mean ± SE, *n* = 2 to 3

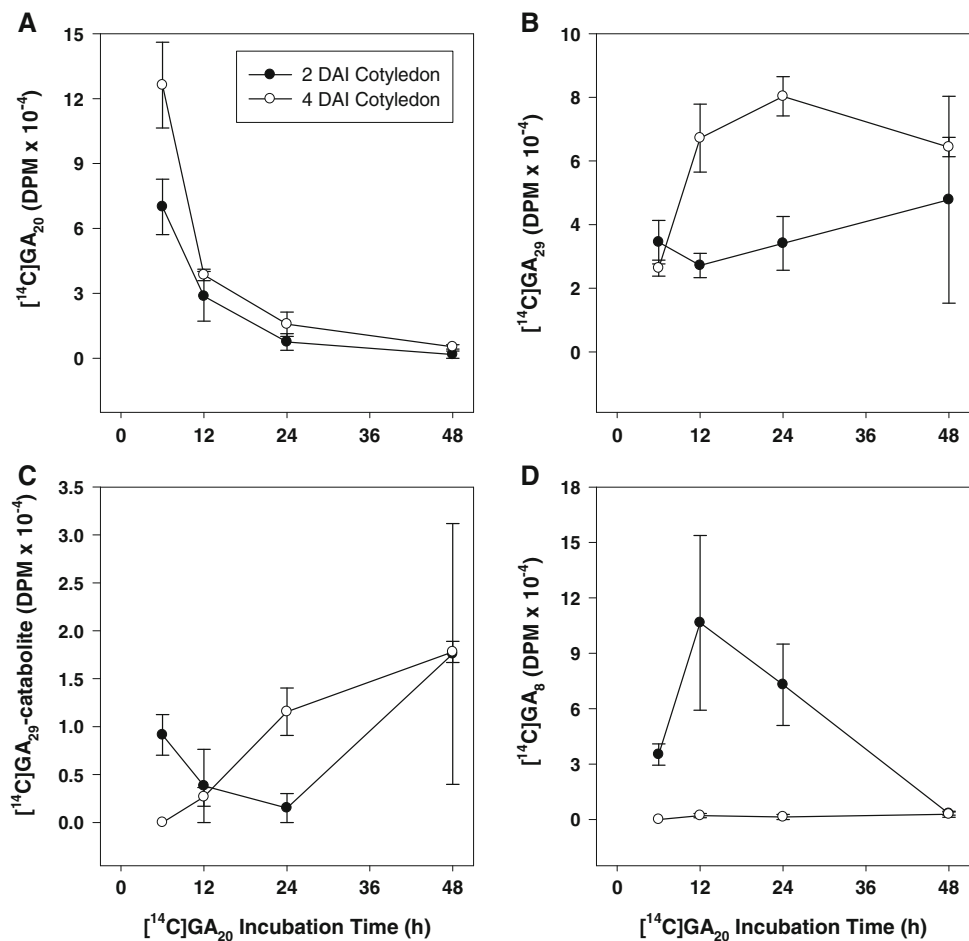
^c Transcript levels were compared across genes, genotypes, and tissues using the average of cotyledonary *PsGA3ox2* samples of ‘Carneval’ as a reference for normalization. Quantitation was performed using an ABI StepOnePlus sequence detector. Due to different PCR efficiencies between the two qRT-PCR models, the abundance of *PsGA3ox1* cannot be directly compared across detectors

whereas [¹⁴C]GA₂₀ was detected in two of three replicates after 24 h, but no [¹⁴C]GA₂₀ was found in roots (Table 5). The presence of [¹⁴C]GA₂₉ and [³H]GA₂₉-catabolite in both the shoot and the root tissue was likely due to metabolism of [¹⁴C]GA₂₀ within these tissues, as grafting and radiolabeled tracer studies indicated that GA₂₀ is the major transported form of GA in pea (Proebsting and others 1992). However, because [¹⁴C]GA₂₀ was metabolized to [¹⁴C]GA₂₉ in the cotyledons (Fig. 2; Table 1) and GA₂₉ is hypothesized to be mobile in the developing seeds (from cotyledons to seed coats; Sponsel 1983), some transport of [¹⁴C]GA₂₉ from the cotyledons to the root and shoots tissues cannot be ruled out. To increase the sensitivity for detection of radiolabeled GA transported to the embryo axis, radiolabeled [³H]GA₂₀ with a higher specific radioactivity was injected into a cotyledon after the other cotyledon was removed from the seedling. Transport of [³H]GA₂₀ to both root and shoot tissues was observed within 12 h of application to the cotyledon (Table 6). Additionally, [³H]GA₂₉ and [³H]GA₂₉-catabolite were the major [³H]GA₂₀ metabolites detected in the shoot and root tissues, with minimal [³H]GA₁ and [³H]GA₈ detected in these tissues. Because [³H]GA₂₀ was consistently

transported to the root and shoot tissues, and 4-DAI shoots have the capacity to metabolize GA₂₀ to GA₂₉ (see below), it is likely that the majority of the [³H]GA₂₀ metabolites found in root and shoot tissues were synthesized after transport of [³H]GA₂₀ into these tissues (Table 6). These data are consistent with the proposed transport of GA₂₀ from cotyledons to the embryo axis as suggested from studies using the *sln* mutant (*sln* seeds have high levels of GA₂₀; Ross and others 1993).

Shoots of ‘Alaska’ treated with [¹⁴C]GA₂₀ were also able to metabolize it to bioactive [¹⁴C]GA₁ (1.7% of the [¹⁴C]GA₂₀ applied to the 4-DAI shoot; Table 7). These metabolic data are consistent with the presence of high *PsGA3ox1* transcript levels (Table 2) and the detection of endogenous GA₁ and its immediate metabolite GA₈ (Table 3) in the shoots of 4-DAI seedlings. The 4-DAI shoots also converted [¹⁴C]GA₂₀ to [¹⁴C]GA₂₉ and [¹⁴C]GA₂₉-catabolite (Table 7). These metabolism data, along with the substantial levels of *PsGA2ox1* mRNA (Table 2) and endogenous GA₂₉ (Table 3) observed in the 4-DAI shoots, suggest that 2β-hydroxylation of GAs is an important mechanism to keep concentrations of bioactive GA in shoots at optimum levels during early seedling

Fig. 2 [^{14}C]GA $_{20}$ (a) and its metabolites [^{14}C]GA $_{29}$ (b), [^{14}C]GA $_{29}$ -catabolite (c), and [^{14}C]GA $_8$ (d) detected over a 48-h period in the cotyledons of 2- or 4-DAI ‘Alaska’ seedlings. [^{14}C]GA $_{20}$ was injected into one cotyledon of the seedling. Data are mean \pm SE, $n = 2$ to 3 (5 cotyledons per n)



growth in pea. Transport of [^{14}C]GA $_{20}$ from the shoot to the root of young (4 DAI) seedlings may also occur because [^{14}C]GA $_{29}$, an immediate metabolite of [^{14}C]GA $_{20}$, was observed in all replicates of root tissues after application of [^{14}C]GA $_{20}$ to the shoot (Table 7); however [^{14}C]GA $_{29}$ transport cannot be ruled out.

Overall, the radiolabeled GA metabolism and transport data, along with the high cotyledonary *PsGA20ox* mRNA abundance (2 DAI, Table 2) and the presence of GA $_{20}$ in the mature embryo (approximately 11 ng gfw $^{-1}$; Table 3), support a working hypothesis that both the GA $_{20}$ sequestered during seed development and the de novo synthesized in the imbibing cotyledons can be transported from the cotyledons to the embryonic axis where it can then serve as a substrate for β -hydroxylation to produce bioactive GA $_1$ required for early seedling growth.

Cultivar Variation in GA Biosynthesis Gene Expression and GA Levels

To broaden our understanding of GA biosynthesis and catabolism during early seedling growth, we compared the expression of GA biosynthesis and catabolism genes and

endogenous GA levels in ‘Alaska,’ a tall (*Le*) vining pea with normal leaf morphology, with that in ‘Carneval,’ a semidwarf (*le-1*) field pea with semileafless morphology, by using an aseptic Petri plate culturing system. ‘Alaska’ had low levels of GA $_1$ in both shoots and roots, whereas ‘Carneval’ had GA $_1$ levels below detection in both shoot and root tissues. A higher GA $_1$ biosynthesis capacity in shoots and roots of ‘Alaska’ than in those of ‘Carneval’ was also supported by the 7- and 26-fold higher GA $_8$ level in ‘Alaska’ shoots and roots, respectively. Additionally, the expression of *PsGA3ox1* and *PsGA2ox2* was about twofold higher in ‘Alaska’ shoots and roots than in ‘Carneval’ tissues. The expression levels of cotyledonary GA biosynthesis genes (*PsGA20ox2* and *PsGA3ox1*) in ‘Carneval’ were three- to fourfold lower than those in ‘Alaska,’ and a more marked variation was evident in the expression of the GA catabolic genes *PsGA2ox1* and *PsGA2ox2* between the two cultivars (Table 2). Specifically, the transcript abundance of *PsGA2ox1* and *PsGA2ox2* in 4-DAI cotyledons of ‘Carneval’ was 6- and 48-fold less, respectively, than that of ‘Alaska’ (Table 2), and this difference in gene expression pattern between the two cultivars was consistent with the endogenous GA profiles at 4 DAI in which ‘Carneval’

Table 3 Endogenous GA levels in mature embryos and in cotyledons, shoots, and roots of 4-DAI seedlings of ‘Alaska’ and ‘Carneval’ grown in a Petri plate

Cultivar	Tissue	Experiment no.	GA ₁₉ ng gfw ⁻¹	GA ₂₀	GA ₂₉	GA ₁	GA ₈
Alaska	Mature embryo	1	1.78	10.84	na	0.07	na
		2	0.05	0.88	339.48	nd	0.54
	Cotyledon	1	0.15	1.64	na	0.13	na
		2	0.61	0.21	243.31	0.11	7.70
	Root	1	1.18	0.73	365.96	0.27	na
		2	0.20	0.18	381.45	0.01	17.90
Carneval	Mature embryo	1	1.18	13.44	277.92	0.12	na
		2	0.15	0.54	27.81	nd	0.10
	Cotyledon	1	1.50	0.22	24.12	nd	0.27
		2	2.00	0.12	28.82	nd	0.30
	Root	1	0.32	0.13	47.81	nd	2.06
		2	0.38	0.12	51.21	nd	2.91
pg organ ⁻¹							
Alaska	Mature embryo	1	375.7	2,285.4	na	15.7	nd
		2	24.0	405.0	156,702.0	nd	250.8
	Cotyledon pair	1	68.9	758.2	na	62.0	na
		2	32.0	11.0	12,652.0	6.0	401.0
	Root	1	61.4	38.0	19,030.0	13.9	na
		2	4.2	3.8	8010.0	0.3	376.0
Carneval	Mature embryo	1	328.1	3,741.2	77,373.3	33.6	na
		2	62.0	215.3	11,178.4	nd	41.0
	Cotyledon pair	1	68.1	9.8	1,097.4	nd	12.1
		2	90.8	5.3	1,311.2	nd	13.6
	Root	1	6.8	2.7	1,008.8	nd	43.4
		2	7.9	2.5	1,080.4	nd	61.4

na not available, nd not detected

cotyledons contained 12-fold less GA₂₉ and 5-fold less GA₈ than those of ‘Alaska’ (Table 3).

A second *GA3ox* gene (*PsGA3ox2*) has been identified recently in pea (Weston and others 2008). To gain insight into the possible role of this gene during germination and early seedling growth, we characterized its expression pattern in both ‘Carneval’ and ‘Alaska’ and compared it to that of *PsGA3ox1*. When compared to *PsGA3ox1*, the transcript abundance of *PsGA3ox2* was very low in all tissues of germinating seeds and actively growing seedlings of both cultivars, suggesting that *PsGA3ox1* encodes for the majority of the GA 3-oxidase activity during early developmental processes in pea (note the different scales for the expression levels of the two genes in vegetative tissues; Fig. 3). We do note, however, that the expression of *PsGA3ox2* was greater in the root than in the shoot of 4- and 6-DAI seedlings in both ‘Alaska’ and ‘Carneval’ (Fig. 3), a finding that is consistent with data reported by Weston and others (2008). The transcript abundance of *PsGA3ox2* in the cotyledons of imbibing pea seeds was

very low during germination and early postgerminative stages, but increased by 4 DAI (Fig. 3c, f). Yaxley and others (2001) postulated that the lack of a root phenotype in *le* mutants was likely due to the presence of a *GA3ox* homolog to *GA3ox1*. Interestingly, during germination and early seedling growth, *PsGA3ox2* remained low in roots of ‘Carneval’ (*le-1* genetic background). Perhaps *PsGA3ox2* expression is upregulated later in root development or in the more severe *le-2* mutant.

Endogenous Auxin Levels

To broaden our understanding of the role of auxins in early seedling growth, the endogenous levels of two naturally occurring auxins, IAA and 4-Cl-IAA, were measured in mature embryos and tissues of aseptically cultured 4-DAI seedlings of ‘Alaska’ and ‘Carneval.’ Rapidly developing pea seeds (~1 week after anthesis) contain high levels of free IAA and 4-Cl-IAA (315–1,570 ng gfw⁻¹ of IAA and 239–720 ng gfw⁻¹ of 4-Cl-IAA; Katayama and others

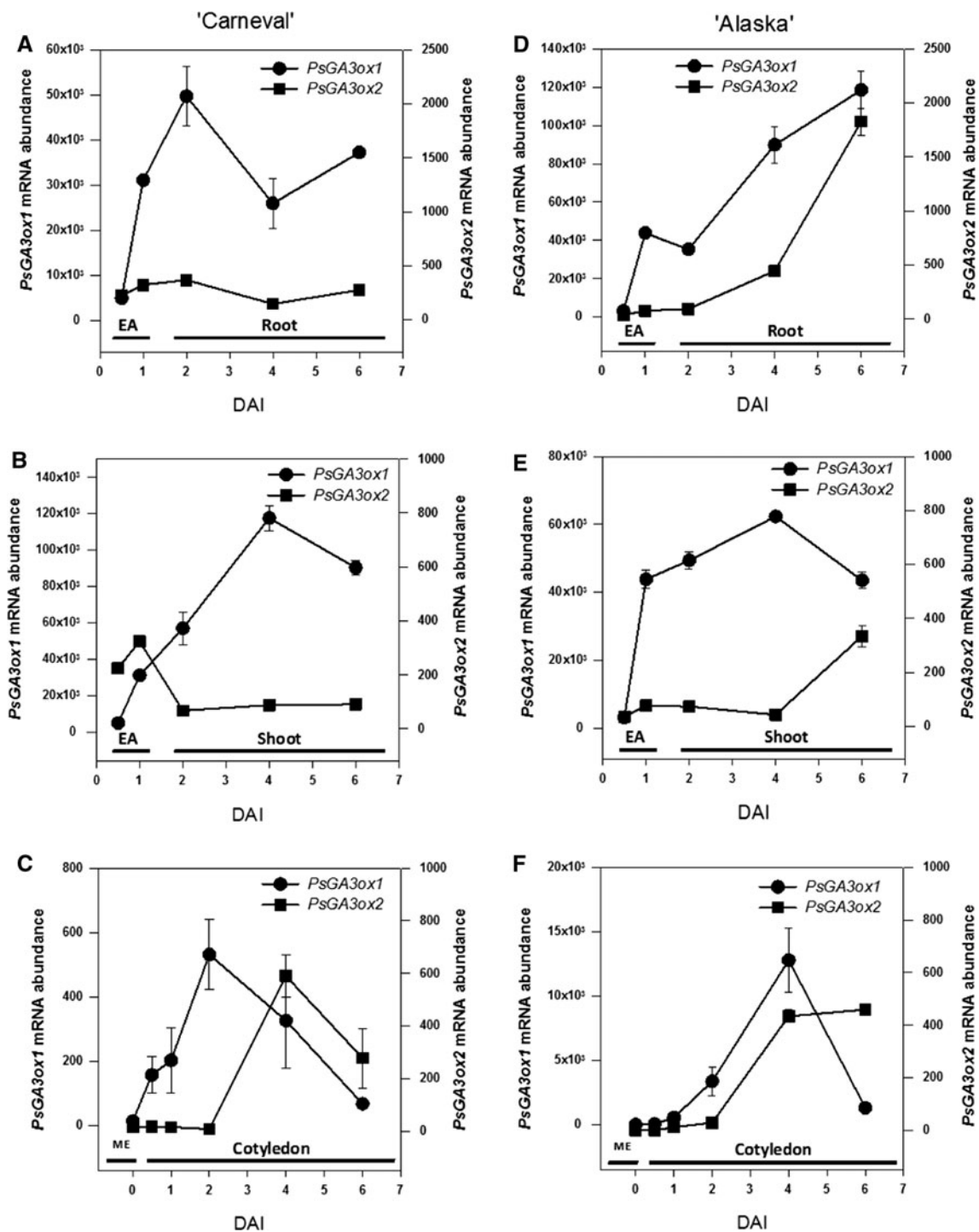


Fig. 3 Relative transcript levels of two GA 3-oxidase genes, *PsGA3ox1* and *PsGA3ox2*, during seed germination and early seedling growth in sand culture of ‘Carneval’ (a–c) and ‘Alaska’ (d–f). Relative transcript levels were determined in mature embryos (ME; c and f), embryo axes (EA; 0.5 and 1 DAI; a, b, d, and e), roots

(2–6 DAI; a and d), shoots (2–6 DAI; b and e), and cotyledons (0.5–6 DAI; c and f) of the imbibed pea seed and growing seedling. Transcript levels were compared across all genes, genotypes, developmental stages, and tissues. Data are mean ± SE, *n* = 2 to 3

1988; Magnus and others 1997), followed by the decrease of both auxins to low levels as the seeds mature (Katayama and others 1988). The IAA and 4-Cl-IAA detected in the

mature embryos (with no testa) of both cultivars (Table 8) represent the residual of the two auxins sequestered at the end of seed maturation. The level of 4-Cl-IAA in the

Table 4 [¹⁴C]GA metabolites in the embryo axis of ‘Alaska’ after 12 h of incubation with [¹⁴C]GA₁₉, [¹⁴C]GA₂₀, or [¹⁴C]GA₁

DAI	[¹⁴ C]GA ₂₀	[¹⁴ C]GA ₁	[¹⁴ C]GA ₂₉	[¹⁴ C]GA ₂₉ -catabolite	[¹⁴ C]GA ₈
[¹⁴C] Metabolite after 12 h of incubation with [¹⁴C]GA₁₉					
0.5	0.6 ± 0.1 ^a (1,763 ± 337) ^b	nd	nd	nd	nd
1	3.0 ± 1.0 (8,360 ± 2,626)	1.1 ^c (3,026)	0.8 ^c (2,217)	1.7 ^c (4,644)	nd
2	1.1 ± 0.6 (3,045 ± 1,620)	nd	nd	nd	nd
[¹⁴C] Metabolite after 12 h of incubation with [¹⁴C]GA₂₀					
0.5		0.6 ± 0.0 (1,467 ± 275)	1.2 ± 0.1 (2,955 ± 304)	nd	0.8 ± 0.3 (1,965 ± 719)
1		nd	6.5 ± 1.0 (15,480 ± 2,297)	nd	0.9 ^c (2,198)
2		nd	2.6 ± 1.0 (6,299 ± 2,528)	nd	0.5 ^c (1,234)
[¹⁴C] Metabolite after 12 h of incubation with [¹⁴C]GA₁					
0.5					1.5 ± 0.1 (3,388 ± 198)
1					2.6 ± 1.5 (5,732 ± 3,390)
2					1.2 ± 0.3 (2,639 ± 542)

The radiolabeled GA was applied to the embryo axis at 0.5, 1, and 2 DAI

nd not detected

^a Values are percentages calculated as (dpm [¹⁴C] metabolite after 12 h of incubation)/(dpm [¹⁴C]GA substrate added to embryo axis) × 100. Data are mean ± SE (*n* = 3; 5 embryo axes per *n*)

^b Values in parentheses are [¹⁴C] metabolite in dpm

^c [¹⁴C]GA metabolite was observed in only one of the three biological replicates

Table 5 [¹⁴C]GA₂₀ and its [¹⁴C]GA metabolites in the shoots and roots of ‘Alaska’ seedlings after [¹⁴C]GA₂₀ was injected into one cotyledon at 4 DAI

Incubation time (h)	[¹⁴ C]GA metabolite				
	[¹⁴ C]GA ₂₀	[¹⁴ C]GA ₂₉	[¹⁴ C]GA ₂₉ -catabolite	[¹⁴ C]GA ₁	[¹⁴ C]GA ₈
Root					
12	nd	0.7 ± 0.1 ^a (2,909 ± 325) ^c	0.5 ^b (2,156)	nd	nd
24	nd	0.5 ± 0.1 (2,062 ± 256)	nd	nd	nd
48	nd	1.4 ± 0.3 (5,632 ± 1,188)	1.0 ± 0.7 (4,053 ± 2,866)	nd	nd
Shoot					
12	1.3 ^b (5,184)	1.2 ± 0.6 (5,014 ± 2,597)	nd	nd	nd
24	0.6 ± 0.3 (2,466 ± 1,026)	2.2 ± 0.1 (8,941 ± 574)	nd	nd	nd
48	nd	4.6 ± 1.7 (18,641 ± 6,718)	nd	nd	nd

nd not detected

^a Values are percentages calculated as (dpm [¹⁴C] metabolite after a given period of incubation)/(dpm [¹⁴C]GA₂₀ injected into the cotyledon) × 100. Data are mean ± SE (*n* = 2 to 3; 5 root or shoot tissues per *n*)

^b [¹⁴C]GA metabolite was observed in only one of the three biological replicates

^c Values in parentheses are [¹⁴C] metabolite in dpm

mature embryos was higher than IAA (4.7-fold in ‘Alaska’ and 9.5-fold in ‘Carneval’; Table 8). The concentration of IAA per gram fresh weight in the cotyledons (the major embryo tissue) increased in ‘Carneval’ and slightly decreased in ‘Alaska’ through 4 DAI (Table 8), when the RWC of the cotyledon increased to 56% (IAA content

increased 1.8-fold in ‘Alaska’ and 5.5-fold in ‘Carneval’ on a gram dry weight basis). Cotyledonary 4-Cl-IAA concentration, on the other hand, decreased during the 4-day imbibition period (8.3-fold in ‘Alaska’ and 6.4-fold in ‘Carneval’ on a gram fresh weight basis; 3.7-fold in both cultivars on a gram dry weight basis; Table 8). The auxin

Table 6 [³H]GA₂₀ and its [³H]GA metabolites detected in the shoot and root tissues of ‘Alaska’ seedlings 12 and 24 h after [³H]GA₂₀ was injected into the remaining cotyledon (after one cotyledon was removed) at 4 DAI

Incubation time (h)	[³ H]GA metabolite				
	[³ H]GA ₂₀	[³ H]GA ₂₉	[³ H]GA ₂₉ -catabolite	[³ H]GA ₁	[³ H]GA ₈
Root					
12	1,576 ± 891 ^a	1,659 ± 793	460 ± 153	80 ± 43	77 ± 42
24	1,324 ± 315	1,027 ± 565	304 ± 62	164 ± 101	86 ± 36
Shoot					
12	1,235 ± 412	3,554 ± 949 ^b	536 ± 196	78 ± 32	119 ± 44 ^b
24	1,742 ± 563	2,945 ± 1754	743 ± 471	136 ± 63	131 ± 77

^a Values are in dpm. Data are mean ± SE (*n* = 3; 5 root or shoot tissues per *n*)

^b Mean ± SE (*n* = 2; 5 root or shoot tissues per *n*)

Table 7 [¹⁴C]GA₂₀, [¹⁴C]GA₁, [¹⁴C]GA₂₉, and [¹⁴C]GA₂₉-catabolite detected in the shoot and root tissues of ‘Alaska’ seedlings 12 h after [¹⁴C]GA₂₀ was applied to the shoot at 4 DAI

Tissue	[¹⁴ C]GA metabolite			
	[¹⁴ C]GA ₂₀	[¹⁴ C]GA ₂₉	[¹⁴ C]GA ₂₉ -catabolite	[¹⁴ C]GA ₁
Shoot	65.5 ± 10.4 ^a (267,434 ± 42,297) ^b	4.8 ± 0.1 (19,717 ± 545)	1.1 ± 0.4 (4,446 ± 1,468)	1.7 ± 0.5 (7,079 ± 1,931)
Root	1.4 ^c (5,841)	1.4 ± 0.5 (5,599 ± 2,191)	0.1 ^c (201)	0.4 ^c (1,628)

^a Values are percentages calculated as (dpm [¹⁴C] metabolite after 12 h of incubation)/(dpm [¹⁴C]GA₂₀ applied to the shoot) × 100. Data are mean ± SE (*n* = 5; 5 root or shoot tissues per *n*)

^b Values in parentheses are [¹⁴C] metabolite in dpm

^c [¹⁴C]GA metabolite was observed in only one of the five biological replicates

content data expressed on a dry weight basis indicate that some IAA is either de novo synthesized or hydrolyzed from IAA conjugates in the cotyledons during this period. For example, in the mature air-dried seeds of ‘Alaska,’ the level of peptidyl-IAA conjugates is twice the level of free IAA (Bandurski and Schulze 1977), and enzymatic hydrolysis of IAA-L-alanine, an IAA conjugate, to free IAA has been reported within 48 h after application of the conjugate into the stem segments of 6–7-day-old ‘Alaska’ seedlings (Hangarter and Good 1981). The decrease of 4-Cl-IAA in cotyledons during germination may be due to increased catabolism or transport of 4-Cl-IAA to the growing embryo axis. Gladish and others (2000) presented evidence that IAA applied to the cotyledons of 2- and 5-day-old pea seedlings was transported into the axes of developing seedlings within 6 h, where the majority (73–81%) of the transport was into the actively growing root. The free IAA and 4-Cl-IAA detected in mature embryos may be used locally during germination, for example, in cotyledon vascularization, or transported to the growing embryo axis for initial seedling development.

Differences in shoot IAA and 4-Cl-IAA content between the two cultivars (each 8-fold greater in ‘Alaska’ than in ‘Carneval’; Table 8) are interesting in the light of their shoot branching patterns. Primary shoot lateral branches

were apparent on 2-week-old ‘Carneval’ seedlings, with an average length of 1.58 cm (± 0.14 SE; *n* = 18) at node 2 (node 0 designated at cotyledon attachments), and with no other lateral branches observed in the next 2 weeks. No lateral shoot branches were evident on ‘Alaska’ seedlings during the same growth period. Furthermore, removal of shoots (plumules) in ‘Alaska’ seedlings resulted in the decrease in the number of lateral root primordia (Table 9). Auxin is thought to be transported from the shoot to the root where it induces lateral root initiation (IAA; McDavid and others 1972). 4-Cl-IAA strongly and IAA moderately stimulated root primordia initiation in pea seedlings of detipped roots (Wightman and others 1980). Indeed, 4-Cl-IAA and IAA treatment to shoot-decapitated ‘Alaska’ seedlings increased lateral root formation (Table 9), supporting that 4-Cl-IAA as well as IAA can be transported from the shoot to the root to initiate lateral rooting. However, roots from ‘Carneval’ seedlings of either intact control or decapitated treated (IAA or 4-Cl-IAA) did not produce any visible lateral root primordia in the aseptic Petri plate culture by 6 DAI (data not shown). ‘Carneval’ seedlings produced lateral roots as did ‘Alaska’ seedlings when both cultivars were cultured in continuous darkness for 4–6 days in the Petri plate system. IAA levels in the shoot and root tissues of both cultivars were markedly

Table 8 IAA and 4-Cl-IAA levels in mature embryos and in cotyledons, roots, and shoots of 4-DAI seedlings of ‘Alaska’ and ‘Carneval’ grown in a Petri plate

Cultivar	Auxin	Mature embryo ng gfw ⁻¹	Seedling tissues		
			Cotyledon	Root	Shoot
Alaska	IAA	3.45	2.86	18.61	15.52
	4-Cl-IAA	16.29	1.97	1.45	1.32
Carneval	IAA	1.08	3.37	19.93	1.94
	4-Cl-IAA	10.30	1.60	1.37	0.16
ng gdw ⁻¹					
Alaska	IAA	3.67	6.64	219.72	105.15
	4-Cl-IAA	17.37	4.57	17.12	8.94
Carneval	IAA	1.39	7.65	269.69	14.55
	4-Cl-IAA	13.26	3.63	18.54	1.20
pg seedling ^{-1a}					
Alaska	IAA	726.2	1,318.1	967.8	326
	4-Cl-IAA	3,434.4	911.3	75.3	27.7
Carneval	IAA	301.8	1,354	907.0	41.0
	4-Cl-IAA	2,868.6	644	62.2	3.5

^a Cotyledon values are calculated per pair of cotyledons

Table 9 Root fresh weight, length, and number of lateral root primordia in control (intact), decapitated, and decapitated and hormone-treated 6-DAI seedlings of ‘Alaska’ grown in a Petri plate

Treatment	Fresh weight (mg)	Primary root length (mm)	Number of lateral root primordia
Control	103.8 ± 10.6 ^a	42.8 ± 4.2	4.5 ± 0.8
Decapitated	117.2 ± 14.0	44.1 ± 4.6	1.2 ± 0.6
Decapitated + IAA (10 ⁻⁶ M)	136.0 ± 9.5	48.4 ± 1.7	1.8 ± 0.4
Decapitated + IAA (10 ⁻⁵ M)	145.6 ± 9.3	47.2 ± 2.8	2.8 ± 0.7
Decapitated + 4-Cl-IAA (10 ⁻⁶ M)	121.3 ± 9.2	47.4 ± 3.3	1.3 ± 0.7
Decapitated + 4-Cl-IAA (10 ⁻⁵ M)	142.1 ± 10.5	47.1 ± 3.6	3.1 ± 0.7

Seedlings were decapitated at 2 DAI by removing the plumules without damaging the cotyledons

^a Data are mean ± SE, *n* = 16 to 20

higher than that of 4-Cl-IAA by 4 DAI (11.8–12.8-fold in ‘Alaska’ and 12.1–14.6-fold in ‘Carneval; Table 8), indicating that IAA is the major form of auxin in the rapidly expanding tissues of young pea seedlings. Because 4-Cl-IAA generally has higher biological activity than IAA (Reinecke 1999), 4-Cl-IAA may have localized roles during seedling development in plants that contain 4-Cl-IAA.

In summary, we provided a working model for GA biosynthesis and metabolism during germination and early seedling growth in pea. Appreciable GA₂₀ is sequestered in the cotyledons at seed maturity. Additionally, during imbibition of pea seeds, *PsGA20ox2* transcripts predominate in the cotyledonary tissue. We postulate that *PsGA20ox2* codes for the de novo synthesis of GA 20-oxidase that results in the production of additional GA₂₀.

This pool of cotyledonary GA₂₀ (initially present and newly synthesized) serves as a substrate for the synthesis of bioactive GA₁ (by GA 3-oxidase encoded by *PsGA3ox* genes) for the cotyledon during germination and also supplies GA₂₀ for transport to both root and shoot tissues of the embryo axis. Transported GA₂₀ supports localized production of bioactive GA₁, which causes the expansion/elongation of the seedling. During early shoot and root expansion, it appears that *PsGA20ox1* encodes for the majority of GA 20-oxidase activity required for the production of GA₂₀, and *PsGA3ox1* encodes for the majority of GA 3-oxidase activity, which catalyzes the synthesis of bioactive GA₁. Finally, changes in the levels of the two naturally occurring auxins, IAA (predominates during young seedling growth) and 4-Cl-IAA (predominates in

mature seed), suggest that these two auxins have different roles during these early developmental processes.

Acknowledgments This work was supported by a grant from the National Sciences and Engineering Research Council of Canada to JAO. The authors thank Jerry Cohen (University of Minnesota) for the heavy-labeled 4-Cl-IAA, Lewis Mander (Australian National University) for the labeled GAs, and Dakshina Pahala-Vithanage for her technical assistance.

References

- Ahmad A, Andersen AS, Engvild K (1987) Rooting, growth and ethylene evolution of pea cuttings in response to chloroindole auxins. *Physiol Plant* 69:137–140
- Ayele BT, Ozga JA, Kurepin LV, Reinecke DM (2006a) Developmental and embryo axis regulation of gibberellin biosynthesis during germination and young seedling growth of pea (*Pisum sativum* L.). *Plant Physiol* 142:1267–1281
- Ayele BT, Ozga JA, Reinecke DM (2006b) Regulation of GA biosynthesis genes during germination and young seedling growth of pea (*Pisum sativum* L.). *J Plant Growth Regul* 25: 219–232
- Bain JM, Mercer FV (1966) Subcellular organization of the cotyledons in germinating seeds and seedlings of *Pisum sativum* L. *Aust J Biol Sci* 19:69–84
- Bandurski RS, Schulze A (1977) Concentration of indole-3-acetic acid and its derivatives in plants. *Plant Physiol* 60:211–213
- Behringer FJ, Davies PJ (1993) The early time course of the inhibition of stem growth of etiolated pea seedlings by fluorescent light. *Plant Growth Regul* 12:341–345
- Bialek K, Cohen JD (1989) Free and conjugated indole-3-acetic acid in developing bean seeds. *Plant Physiol* 91:775–779
- Brian PW, Hemming HG (1955) The effect of gibberellic acid on shoot growth of pea seedlings. *Physiol Plant* 8:669–681
- Chawla R, DeMason DA (2004) Molecular expression of *PsPIN1*, a putative auxin efflux carrier gene from pea (*Pisum sativum* L.). *Plant Growth Regul* 44:1–14
- Chen F, Dahal P, Bradford KJ (2001) Two tomato expansin genes show divergent expression and localization in embryos during seed development and germination. *Plant Physiol* 127: 928–936
- Dharmasiri N, Dharmasiri S, Weijers D, Lechner E, Yamada M, Hobbie L, Ehrismann JS, Jurgens G, Estelle M (2005) Plant development is regulated by a family of auxin receptor f box proteins. *Dev Cell* 9:109–119
- Epstein E, Cohen JD, Bandurski RS (1980) Concentration and metabolic turnover of indoles in germinating kernels of *Zea mays* L. *Plant Physiol* 65:415–421
- Gaskin P, MacMillan J (1991) GC–MS of the gibberellins and related compounds: methodology and a library of spectra. Cantock's Enterprise, Bristol
- Gladish DK, Sutter EG, Rost TL (2000) The role of free indole-3-acetic acid (IAA) levels, IAA transport, and sucrose transport in the high temperature inhibition of primary root development in pea (*Pisum sativum* L. cv. Alaska). *J Plant Growth Regul* 19:347–358
- Graebe JE (1986) Gibberellin biosynthesis from gibberellin A₁₂-aldehyde. In: Bopp M (ed) *Plant growth substances* 1985. Springer-Verlag, New York, pp 74–82
- Groot SPC, Karssen CM (1987) Gibberellins regulate seed germination in tomato by endosperm weakening: a study with gibberellin mutants. *Planta* 171:525–531
- Hangarter RP, Good NE (1981) Evidence that IAA conjugates are slow release sources of free IAA in plant tissues. *Plant Physiol* 68:1424–1427
- Hedden P, Phillips AL (2000) Gibberellin metabolism: new insights revealed by the genes. *Trends Plant Sci* 5:523–530
- Katayama M, Thiruvikraman SV, Marumo S (1988) Localization of 4-chloroindole-3-acetic acid in seeds of *Pisum sativum* and its absence from all other organs. *Plant Cell Physiol* 29:889–891
- Koornneef M, van der Veen JH (1980) Induction and analysis of gibberellin sensitive mutants in *Arabidopsis thaliana* (L.) Heynh. *Theor Appl Genet* 58:257–263
- Livak KJ, Schmittgen TD (2001) Analysis of relative gene expression data using real-time quantitative data using real-time quantitative PCR and the 2^{-ΔΔC_t} method. *Methods* 25:402–408
- Magnus V, Ozga JA, Reinecke DM, Pierson GL, Larue TA, Cohen JD, Brenner ML (1997) 4-Chloroindole-3-acetic and indole-3-acetic acids in *Pisum sativum*. *Phytochemistry* 46:675–681
- McDavid CR, Sagar GR, Marshall C (1972) The effect of auxin from the shoot on root development in *Pisum sativum* L. *New Phytol* 71:1027–1032
- Ogawa M, Hanada A, Yamauchi Y, Kuwahara A, Kamiya Y, Yamaguchi S (2003) Gibberellin biosynthesis and response during *Arabidopsis* seed germination. *Plant Cell* 15:1591–1604
- Ozga JA, Reinecke DM (2003) Hormonal interactions in fruit development. *J Plant Growth Regul* 22:73–81
- Ozga JA, Reinecke DM, Ayele BT, Ngo P, Nadeau C, Wickramaratna AD (2009) Developmental and hormonal regulation of gibberellin biosynthesis and catabolism in pea fruit. *Plant Physiol* 150:448–462
- Park S, Ozga JA, Cohen JD, Reinecke DM (2010) Evidence of 4-Cl-IAA and IAA bound to proteins in pea fruit and seeds. *J Plant Growth Regul* 29:184–193
- Proebsting WM, Hedden P, Lewis MJ, Croker SJ, Proebsting LN (1992) Gibberellin concentration and transport in genetic lines of pea: effects of grafting. *Plant Physiol* 100:1354–1360
- Rampey RA, LeClere S, Kowalczyk M, Ljung K, Sandberg G, Bartel B (2004) A family of auxin-conjugate hydrolases that contributes to free indole-3-acetic acid levels during *Arabidopsis* germination. *Plant Physiol* 135:978–988
- Reid JB, Ross JJ, Swain SM (1992) Internode length in *Pisum*: a new, slender mutant with elevated levels of C₁₉ gibberellins. *Planta* 188:462–467
- Reinecke DM (1999) 4-Chloroindole-3-acetic acid and plant growth. *Plant Growth Regul* 27:3–13
- Ross JJ, Reid JB, Swain SM (1993) Control of stem elongation by gibberellin A₁: evidence from genetic studies including the slender mutant *sln*. *Aust J Plant Physiol* 20:585–599
- Ross JJ, O'Neill DP, Smith JJ, Kerckhoffs LHJ, Elliott RC (2000) Evidence that auxin promotes gibberellin A₁ biosynthesis in pea. *Plant J* 21:547–552
- Schneider EA, Kazakoff CW, Wightman F (1985) Gas chromatography-mass spectrometry evidence for several endogenous auxins in pea seedling organs. *Planta* 165:232–241
- Silva T, Davies PJ (2007) Elongation rates and endogenous indole-acetic acid levels in roots of pea mutants differing in internode length. *Physiol Plant* 129:804–812
- Smith DL, Flinn AM (1967) Histology and histochemistry of the cotyledons of *Pisum arvense* L. during germination. *Planta* 74:72–85
- Sponsel VM (1983) The localization, metabolism and biological activity of gibberellins in maturing and germinating seeds of *Pisum sativum* cv. *Progress No. 9*. *Planta* 159:454–468
- Sponsel VM (1995) The biosynthesis and metabolism of gibberellins in higher plants. In: Davies PJ (ed) *Plant hormones: physiology, biochemistry and molecular biology*. Kluwer Academic, Dordrecht, pp 66–97

- Tanimoto E (1988) Gibberellin regulation of root growth with change in galactose content of cell walls in *Pisum sativum*. *Plant Cell Physiol* 29:269–280
- van Huizen R, Ozga JA, Reinecke DM (1997) Seed and hormonal regulation of gibberellin 20-oxidase expression in pea pericarp. *Plant Physiol* 115:123–128
- Weston DE, Elliott RC, Lester DR, Rameau C, Reid JB, Murfet IC, Ross JJ (2008) The pea DELLA proteins LA and CRY are important regulators of gibberellin synthesis and root growth. *Plant Physiol* 147:199–205
- Wightman F, Schneider EA, Thimann KV (1980) Hormonal factors controlling the initiation and development of lateral roots. II. Effects of exogenous growth factors on lateral root formation in pea roots. *Physiol Plant* 49:304–314
- Yaxley JR, Ross JJ, Sherriff LJ, Reid JB (2001) Gibberellin biosynthesis mutations and root development in pea. *Plant Physiol* 125:627–633